

Accepted Manuscript

Title: Amylase binding to starch granules under hydrolysing and non-hydrolysing conditions

Author: Sushil Dhital Frederick J. Warren Bin Zhang Michael J. Gidley



PII: S0144-8617(14)00639-0
DOI: <http://dx.doi.org/doi:10.1016/j.carbpol.2014.06.063>
Reference: CARP 9028

To appear in:

Received date: 24-12-2013
Revised date: 13-6-2014
Accepted date: 16-6-2014

Please cite this article as: Dhital, S., Warren, F. J., Zhang, B., and Gidley, M. J., Amylase binding to starch granules under hydrolysing and non-hydrolysing conditions, *Carbohydrate Polymers* (2014), <http://dx.doi.org/10.1016/j.carbpol.2014.06.063>

This is a PDF file of an unedited manuscript that has been accepted for publication. As a service to our customers we are providing this early version of the manuscript. The manuscript will undergo copyediting, typesetting, and review of the resulting proof before it is published in its final form. Please note that during the production process errors may be discovered which could affect the content, and all legal disclaimers that apply to the journal pertain.

1 **Amylase binding to starch granules under hydrolysing and non-**
2 **hydrolysing conditions**

3 Sushil Dhital^{1,2}, Frederick J. Warren², Bin Zhang^{1,2}, Michael J. Gidley^{1,2*}

4

5 ¹ ARC Centre of Excellence in Plant Cell Walls, Centre for Nutrition and Food Sciences,
6 Queensland Alliance for Agriculture and Food Innovation, The University of Queensland, St
7 Lucia, Qld 4072, Australia.

8 ² Centre for Nutrition and Food Sciences, Queensland Alliance for Agriculture and Food
9 Innovation, The University of Queensland, St Lucia, Qld 4072, Australia.

10

11

12

13

14

15

16

17 * Corresponding author.

18 Phone: +61 7 3365 2145; Fax: +61 7 3365 1177. Email address: m.gidley@uq.edu.au (M. J.

19 Gidley)

20

21 **Abstract**

22 Although considerable information is available about amylolysis rate, extent and pattern of
23 granular starches, the underlying mechanisms of enzyme action and interactions are not fully
24 understood, partly due to the lack of direct visualisation of enzyme binding and subsequent
25 hydrolysis of starch granules. In the present study, α -amylase (AA) from porcine pancreas
26 was labelled with either fluorescein isothiocyanate (FITC) or tetramethylrhodamine
27 isothiocyanate (TRITC) fluorescent dye with maintenance of significant enzyme activity. The
28 binding of FITC/TRITC-AA conjugate to the surface and interior of granules was studied
29 under both non-hydrolysing (0 °C) and hydrolysing (37 °C) conditions with confocal
30 microscopy. It was observed that enzyme binding to maize starch granules under both
31 conditions was more homogenous compared with potato starch. Enzyme molecules appear to
32 preferentially bind to the granules or part of granules that are more susceptible to enzymic
33 degradation. The specificity is such that fresh enzyme added after a certain time of incubation
34 binds at the same location as previously bound enzyme. By visualising the enzyme location
35 during binding and hydrolysis, detailed information is provided regarding the heterogeneity
36 of granular starch digestion.

37

38 **Keywords:** Alpha-amylase, starch granules, confocal microscopy, enzyme binding, surface
39 structure

40

41 **1 Introduction**

42 Starch is a major component in the human diet, as well as a feedstock for a range of industrial
43 processes. The enzymic hydrolysis of starches to smaller oligomers either in living organisms
44 or industrial processes involves the action of α -amylase (AA), an endo-acting enzyme that
45 hydrolyses α -1 \rightarrow 4 glycosidic bonds of amylose or amylopectin molecules. The amylolysis
46 rate, extent and pattern of starch granules vary depending upon the barriers the enzyme
47 encounters to access and then bind to the starch granules; or upon structural features of starch
48 granules that prevent catalysis after initial binding. These mechanisms have been recently
49 reviewed (Dhital, Warren, Butterworth, Ellis & Gidley, 2013).

50 Studies of starch hydrolysis either *in vivo* or *in vitro* inevitably provide an average value from
51 a population of starch granules. Recent evidence, however, indicates that there is a great deal
52 of heterogeneity in the internal architecture (Dhital, Shelat, Shrestha & Gidley, 2013) and
53 physical and chemical structures (Liu et al., 2013) within individual granules. This could in
54 principle affect enzyme binding and ultimately the catalytic process.

55 Studies of amylase binding to starch granules by solution depletion assay at 0 °C, found a
56 dependence of enzyme affinity for starch on the surface area, and therefore particle size of
57 starch granules (Schwimmer & Balls, 1949; Walker & Hope, 1963; Warren, Royall,
58 Gaisford, Butterworth & Ellis, 2011). Due to the lack of visualisation of enzyme bound to the
59 granules, it could not be determined from these studies whether the enzyme was uniformly
60 bound to all granules or preferentially bound to individual granules with special granular
61 structures.

62 The morphological changes of starch granules during α -amylolysis have been investigated by
63 analysis of remnant undigested granules by using various microscopic techniques such as
64 light (bright or polarised field) (Leach & Schoch, 1961), scanning electron (Planchot,
65 Colonna, Gallant & Bouchet, 1995), transmission electron (Gallant, Bouchet & Baldwin,
66 1997), atomic force (Sujka & Jamroz, 2009) and confocal laser scanning (Apinan et al., 2007;
67 Lynn & Cochrane, 1997) microscopy. The α -amylolysis patterns of starches from different
68 botanical origins have been described, for example, cereal starches are hydrolysed from the
69 inside of granules towards the periphery (endo-corrosion, inside-out or centrifugal hydrolysis
70 pattern); whereas high-amylose and tuber starches are hydrolysed from the surface towards
71 the interior of granules (exo-corrosion, outside-in, or centripetal hydrolysis pattern). These
72 differences in digestion pattern have been inferred to be related to the surface features of
73 granular starch, possibly reflecting the presence of pores and channels within cereal starches
74 that allow amylase to penetrate towards the less organised granule interior compared to the
75 rigid and smooth surface and interior of tuber starches (Huber & BeMiller, 1997; Jane &
76 Shen, 1993; Pan & Jane, 2000). Although these techniques provide general information
77 regarding the hydrolysis pattern, they do not allow the visualisation of enzyme at the sites of
78 hydrolysis.

79 Previous authors have attempted to visualise the location of enzyme molecules hydrolysing
80 inside granules. Thomson *et al.* (1994) carried out real-time atomic force microscopic (AFM)
81 imaging of wheat starch degradation by α -amylase. The AFM method is, however, limited to
82 observations of the granule surface, and could not directly visualise the location of enzyme
83 molecules. Similarly, Helbert *et al.* (1996) studied the degradation of starch granules with
84 direct localisation of the amylase by immunogold-labelling. The method, however, was
85 unable to quantify the gold labelling efficiency of enzymes. Furthermore, the cross-sectioning
86 of granules for electron microscopic observation may induce artefacts, for example cracks

87 resembling the channels. Most recently, Tawil *et al.* (2010) used synchrotron ultraviolet
88 fluorescence microscopy to visualize the adsorption and diffusion of amylase during starch
89 degradation. The technique directly visualised the location of protein by imaging the auto-
90 fluorescence from tryptophan present in AA. This method, while a powerful technique, can
91 only visualise one granule at a time, rather than whole populations of granules. Furthermore,
92 fluorescence from AA cannot be discriminated from other granule associated protein
93 components.

94 Thus different aspects of the mechanism of amylase reaction with starch granules have been
95 proposed as the outcome of observation using different techniques. However, there are a
96 number of questions which remain unresolved:

- 97 1. Do enzymes bind uniformly to the granule surface?
- 98 2. Do the surface structure and botanical origin of starch granules affect amylase
99 binding?
- 100 3. Why is there heterogeneity in starch granule digestion?
- 101 4. Is the heterogeneity of starch granules digestion related to enzyme binding?
- 102 5. Do surface features such as pores and channels enhance the diffusion of amylase
103 inside the granules?

104 The present paper aims to address these questions based on the outcomes of direct
105 localisation of fluorescein isothiocyanate (FITC) and tetramethylrhodamine isothiocyanate
106 (TRITC) labelled AA during binding (under both non-hydrolysing (0 °C) and hydrolysing (37
107 °C) conditions) of starch granules from different botanical origins using confocal microscopy.
108 The role of surface pores and channels towards amylase action was further studied through

109 visualization of the diffusion of fluorescent dextran probes followed by diffusion of labelled
110 AA into starch granules.

111 **2 Materials and Methods**

112 **2.1 Materials**

113 Potato starch (PS, Sigma S4251) was purchased from Sigma-Aldrich, Australia. Three types
114 of maize starches: high amylose maize starch (Gelose 80) (HAMS, G80), regular maize
115 starch (MS) and waxy maize starch (WMS) were purchased from Penford Australia Ltd.,
116 (Lane Cove, Sydney, Australia).

117 **2.2 α -Amylase labelling with FITC and TRITC**

118 α -Amylase from porcine pancreas (A6255, Sigma) was labelled with FITC (F7250, Sigma)
119 and TRITC (87918, Sigma) at 10 \times molar excess in carbonate buffer (0.1M, pH 9) following
120 the method of The & Feltkamp (1970). The unbound FITC from the conjugate was separated
121 using a desalting column (Sephadex, PD-10) with phosphate buffered saline buffer (PBS,
122 P4417, Sigma, pH 7.2). Following labelling, the enzyme solution was immediately aliquoted
123 and frozen for storage. The enzyme was defrosted immediately prior to use. Freezing did not
124 affect the enzyme activity. The dye: protein (F/P) molar ratio is defined as the ratio of moles
125 of fluorescent moiety to moles of protein in the conjugate (The & Feltkamp, 1970), and was
126 2.36 and 4.67 for the FITC- and TRITC-AA conjugates respectively. A unit of activity was
127 defined as the enzyme required to liberate 1.0 mg of maltose from starch in 3 minutes at pH
128 6.9 and 37 °C, and activity was found to be 1078 and 1713 unit/mg of protein for FITC and
129 TRITC conjugates respectively, compared to 2485 unit/mg of protein for the unlabelled
130 enzyme. The protein concentration of FITC, TRITC and unlabelled enzyme stock solutions
131 was 1.39, 2.56 and 29 mg/mL, respectively.

132 Michaelis-Menten kinetic parameters for unlabelled and FITC labelled AA were determined
133 using MS as a substrate, using a modification of the method of Tahir *et al.* (2010). Briefly, 4
134 mL of various concentrations of starch (2.5-25 mg/mL) in PBS buffer were incubated at 37
135 °C in a water bath. At time 0, enzyme was added to a concentration of 1.5 nM. At 0, 4, 8 and
136 12 min, 300 μ L of starch suspension was removed and immediately added to 300 μ L of 0.3
137 M Na_2CO_3 in a microcentrifuge tube to stop the reaction. These samples were then
138 centrifuged at 16,000 g for 5 min to remove unreacted starch, and 300 μ L of supernatant
139 removed to a fresh microfuge tube. The reducing sugar content was measured by the *para*-
140 hydroxybenzoic acid hydrazide (PAHBAH) assay (H9882, Sigma) as described by Moretti &
141 Thorson (2008) and expressed as maltose reducing sugar equivalents. Kinetic parameters
142 were obtained from non-linear regression analysis using Sigmaplot[®] 12.5. All kinetic analysis
143 was carried out in triplicate.

144 **2.3 Confocal laser scanning microscopy**

145 Unless otherwise stated, labelled α -amylase (FITC-AA and TRITC-AA) was observed using
146 a confocal microscope (LSM 700, Carls Zeiss, Germany) with a Plan-Apochromat 20 \times lens
147 (with digital zoom of 2 \times for maize, waxy maize), with and without differential interference
148 contrast (DIC) using Zen Black 2011 software (Carl Zeiss Version 7.1). Starch images were
149 taken using a frame size of 1024 \times 1024 at a scan speed of 8 bit and a pixel dwell time of
150 1.58 μ s, from an optical slice of 2 μ m thickness. All imaging was performed with a 10 mW
151 argon ion laser at 2% power with excitation of 488 nm and 555 nm for FITC and TRITC
152 respectively, either singly or in combination.

153 **2.4 Enzyme binding to starch granules at 0 °C**

154 The binding of FITC- and TRITC-AA conjugates to MS and PS granules was monitored at 0
155 °C. A 10 mg/mL starch granule dispersion (2 mL) in sodium acetate buffer (0.2 M, pH 6.0) in
156 10 mL flat bottom tubes (97×16 mm) was immersed fully in an ice water bath placed above a
157 stirrer plate. The dispersion was equilibrated for 10 min with continuous stirring at 200 rpm
158 to ensure that the starch suspension obtained a temperature of 0 °C. The binding experiment
159 was carried out in three different combinations. In the first set, 0.8 unit of FITC-AA
160 conjugate per mg of starch was added and 100 µL aliquots were transferred to 1.5mL
161 microfuge tubes after 5, 10 and 20 min of incubation. Subsequently, 0.8 units TRITC-AA
162 conjugate per mg of starch was added to the same incubation tube and aliquots were taken 5,
163 10 and 20 min after addition of the second enzyme. In a second set, TRITC-AA conjugate
164 was added first followed by FITC-AA conjugate as described for the first set. In a third set,
165 both FITC and TRITC-AA conjugates were added simultaneously.

166 Aliquots were immediately centrifuged at 2000 g for 30 s, supernatants discarded, and the
167 starch pellet observed using the confocal microscope as described in section 2.3.

168 **2.5 Enzyme binding to porous starch**

169 In order to evaluate the roles of surface pores and channels in enzyme binding, porous starch
170 granules were obtained by hydrolysing 3 mL of 1% maize starch suspension with 0.8 units
171 per mg of AA (un-labelled) for 20 min at 37 °C. The reaction was halted by the addition of 10
172 mL of absolute ethanol. The tube was centrifuged at 2000 g for 5 min. The pellet was washed
173 3 times with deionised water and the volume adjusted to 3 mL with acetate buffer (0.2M, pH
174 6.0). The tube was then incubated at 0 °C for 10 min under the same mixing condition (200
175 rpm), and the binding experiment was carried out as described in section 2.4.

176 **2.6 Evaluation of the role of pores and channels during initial amylolysis**

177 To evaluate the role of pores (and channels) in the initial stages of amylolysis, 250 μL (2
178 mg/mL in distilled water) of average molecular weight >65000 Da TRITC dextran (Sigma,
179 T1162) was mixed with 5 mL of 10 mg/mL MS in acetate buffer (0.2 M, pH 6.0) with 0.02%
180 (w/v) sodium azide overnight at 37 °C under stirring (200 rpm). The FITC-AA conjugate (0.8
181 unit/mg of starch) was added to the solution and incubated for 1 h under the same condition.
182 Aliquots (50 μL) were taken after 5, 30 and 60 min. The diffusion of dextran probes inside
183 maize starch granules and the status of diffused probes following further amylolysis were
184 assessed by observing the granules after centrifugation as described in sections 2.3 and 2.4.

185 **2.7 Enzymic digestion of granular starches**

186 Enzymic digestion was carried out using 0.1, 0.4 and 0.8 unit of FITC-AA conjugate per mg
187 of starch (WMS, MS, PS or HAMS). Starch suspension (5 mL, 10 mg/mL) in acetate buffer
188 (0.2M, pH 6, containing 0.02% (w/v) sodium azide) was incubated with FITC-AA conjugate
189 and mixed at 37 °C. At set times between 5 and 1440 min of incubation, aliquots (100 μL)
190 were transferred into 1.5 mL microcentrifuge tubes and immediately centrifuged at 2000 g for
191 30 s. The supernatant was used to determine the reducing sugar content using the PAHBAH
192 assay as described by Moretti & Thorson (2008), and starch pellets from 0.1 and 0.8 unit of
193 FITC-AA conjugate were used for confocal microscopic observation. Pellets from 0.8 unit of
194 FITC-AA conjugate were also oven dried at 40 °C overnight for electron microscopic
195 observation.

196 **2.8 Scanning electron microscopy**

197 The oven-dried samples were thinly spread onto circular metal stubs covered with double-
198 sided adhesive carbon tape, and then platinum coated in a Sputter coater (Eiko IB3, Mito,
199 Japan). Images of the granules were acquired with a JEOL 6300 scanning electron

200 microscope (JEOL Ltd., Tokyo, Japan) under an accelerating voltage of 5 kV. Multiple
201 micrographs of each sample were examined at multiple magnifications and typical
202 representative images selected.

203 **3 Results**

204 **3.1 Kinetic analysis of FITC labelled and unlabelled α -amylase**

205 Michaelis-Menten kinetic parameters were obtained for both the FITC labelled and
206 unlabelled enzymes. The V_{\max} value was found to drop from 30.50 (\pm 3.10) to 15.27 (\pm 1.65)
207 μ M/min following labelling of the enzyme, indicating that the addition of the FITC
208 significantly reduced the catalytic activity of the enzyme. The K_m value, however, was
209 relatively unchanged following labelling, with a value of 12.94 (\pm 2.67) and 17.30 (\pm 3.52)
210 mg/mL for the unlabelled and labelled enzyme respectively. Thus, while the labelling had a
211 large effect on the enzyme's catalytic rate, substrate binding was far less affected. This
212 indicated that the labelled enzyme was still able to bind to starch with an affinity similar to
213 the unlabelled form.

214 **3.2 α -Amylase binding to native starch granules**

215 Representative confocal microscopic images of FITC and TRITC-AA conjugates bound to
216 MS after 5 and 20 min of incubation under non-hydrolysing condition (0 °C) are shown in
217 **Figure 1A**, and clearly reflect the heterogeneity of AA (both FITC and TRITC) binding to
218 MS granules.

219 Double labelling of maize starch, using FITC-AA conjugate followed by TRITC-AA
220 conjugate, is shown in **Figure 1B**. It can be observed that the TRITC-AA conjugate added
221 after 20 min of incubation at 0 °C, binds to exactly the same granules at the same locations, as
222 the FITC-AA conjugate was bound previously. In some granules (as marked), FITC-AA

223 conjugate was observed in the core of granules as well as the surface, while TRITC-AA,
224 which has had less incubation time, is only bound at the granule surface.

225 Double labelling of TRITC-AA followed by FITC-AA, as presented in supplementary
226 information **Figure S1**, followed a similar pattern as shown in **Figure 1B**. Labelling of FITC-
227 AA simultaneously with TRITC-AA on maize starch granules is presented in supplementary
228 information **Figure S2**. Similar to sequential labelling, one subsequent to the other, when
229 used together the two conjugates also show the heterogeneous, but preferential binding
230 towards specific maize granules.

231 Similar to MS, **Figure 1C** shows the heterogeneity of FITC- and TRITC-AA conjugates
232 binding to the surface of PS granules. The binding is more heterogeneous in PS compared to
233 MS, with apparently a smaller fraction of the granules showing fluorescence after both 5 and
234 20 min incubation time. In contrast to MS, binding was mostly limited to the outer
235 circumference of PS granules. Binding was not observed to be dependent on granule size.

236 Double labelling of PS, FITC-AA conjugate followed by TRITC-AA conjugate, is shown in
237 **Figure 1D**. Specificity of binding location to PS was also observed similar to that of MS.
238 TRITC-AA conjugate added after 20 min of incubation at 0 °C, bound to the same
239 granules/location where FITC-AA conjugate was bound previously. The double labelling of
240 TRITC-AA followed by FITC-AA, as presented in supplementary information **Figure S3**,
241 also followed a similar pattern to that of individual labelling as shown in **Figure 1C**.
242 Similarly, double labelling of FITC-AA and TRITC-AA together on PS granules is presented
243 in supplementary information **Figure S4**. In parallel to double labelling, one followed by the
244 other, the two conjugates added simultaneously also showed heterogeneous, but preferential,
245 binding to specific PS granules.

246 **3.3 Amylase binding to enzyme treated (porous) starch granules**

247 In order to study the effect of starch porosity on amylase binding, porous MS was obtained
248 by partial hydrolysis with 0.8 unit of unlabelled amylase per mg of starch for 20 min as
249 described in section 2.2.4. Numerous pores on the surface of maize starch granules were
250 observed after 20 min of hydrolysis as seen in **Figure 2A**. Though limited by magnification
251 and resolution, channels extending towards the granule interior can be seen in the confocal
252 microscopic picture (**Figure 2B**). The confocal and differential interference contrast images
253 after 5 min incubation of porous starch with the FITC-AA conjugate are shown in **Figure 2C**.
254 Compared to non-porous granules (**Figure 1A**), amylase can freely diffuse inside the porous
255 granules as observed by the higher intensity of the FITC-AA conjugate in the granule interior
256 (marked by the solid arrow in **Figure 2D**). For non-porous or less porous granules, enzyme
257 was concentrated in the outer surfaces, as marked by the dotted arrow in **Figure 2D**, similar
258 to what was observed for untreated MS in **Figure 1A**.

259 **3.4 Diffusion of dextran probes and initial amylolysis of starch granules**

260 As shown in **Figure 3B** and **C**, following an overnight incubation with TRITC labelled
261 dextran, a small number of granules have (red) dextran probes inside them (shown by arrows
262 in **Figure 3B** and **C**). After 5 min amylolysis, granules are observed with varying degrees of
263 hydrolysis (damage) with the green fluorescence (FITC-AA conjugate) bound either to the
264 interior or the peripheral regions of the granules (**Figure 3 D, E and F**). TRITC dextran was
265 still observed in some granules, but there was not an obvious co-localization between TRITC
266 dextran and FITC-AA (shown by arrows in **Figure 3E** and **F**). After incubation for 30 and 60
267 min, however, the TRITC dextran was not observed, suggesting that starch hydrolysis by the
268 amylase had resulted in release of the labelled dextran.

269 **3.5 Amylolysis of granular starches**

270 The digestion progress curves of MS and PS with 0.1, 0.4, and 0.8 unit of FITC-AA
271 conjugate are shown in **Figure 4**. As expected, the extent of hydrolysis is dependent upon the
272 concentration of enzyme applied, as the substrate concentration is constant in all cases. The
273 hydrolysis extent of starches followed the order of WMS>MS>PS>HAMS at all the enzyme
274 concentrations used in the experiment.

275 The hydrolysis pattern observed by electron microscopy is shown in **Figures 5** and **6**, and
276 supplementary information **Figures S5, S6** for MS, PS, WMS and HAMS (Gelose 80)
277 respectively. A-type polymorphic starches (WMS and MS) were hydrolysed by formation
278 and enlargement of pores during the digestion time course, whereas B-polymorphic starches,
279 PS and HAMS, were hydrolysed from the surface of the granules towards the interior.

280 Confocal and differential interference contrast images of hydrolysed MS and PS (0.8 units
281 FITC-AA conjugate per mg of starch) are presented in **Figure 7**. Similarly, confocal and
282 differential interference contrast images of MS and PS incubated with 0.1 units FITC-AA
283 conjugate per mg of starch, and WMS and HAMS at both enzyme concentrations are
284 presented in supplementary information **Figures S7, S8** and **S9** respectively. The digestion
285 pattern of MS with labelled enzymes was observed to be heterogeneous. In the initial 5 min
286 of incubation, separate populations of high and low enzyme labelled granules were observed.
287 On further incubation to 2 h, in contrast to the initial heterogeneous binding, almost all of the
288 granules (**Figure 7**) showed bound FITC-AA conjugate, with only a few exceptions. Electron
289 microscopy also showed that almost all the MS granules after 2 h incubation were similarly
290 porous. In contrast to MS, more selective enzyme binding of FITC-AA conjugate to digested
291 residues of PS was observed (**Figure 7**). This is in accordance with SEM observations, where
292 only a few PS granules were eroded during the digestion time course. Enzyme binding was
293 found to be concentration dependent; at higher enzyme concentrations (0.8 units per mg of

294 starch) comparatively more granules were observed with bound enzyme compared to a lower
295 enzyme concentration (0.1 units per mg of starch). Binding was still observed to be
296 preferential (heterogeneous) even at higher enzyme concentrations.

297 For MS and WMS, the enzyme which initially bound to the outer surface, subsequently
298 diffused towards the granule interior with longer incubation times (**Figures 7**, supplementary
299 information **Figure S7, S8**). For example, the intensity and number of granules with internal
300 fluorescence after 2 h of incubation time was comparatively higher than that at 30 min
301 incubation. In contrast, the diffusion of enzyme inside PS and HAMS granules was not
302 observed. They were digested from the outer surface towards the interior. Even after 24 h
303 incubation time, a few granules were highly eroded with enzyme bound at the erosion
304 surfaces whereas the rest were intact without any substantial enzyme binding (**Figure 7**).

305 **4 Discussion**

306 For the first time, we have been able to identify the location of bound amylase to starch
307 granules under both non-hydrolysing and hydrolysing conditions. The results obtained lead us
308 to propose that the heterogeneity of amylase action on starch granules during hydrolysis is
309 due to preferential or selective binding of amylase to the granule surface. The possible
310 reasons for the preferential binding are discussed below.

311 **4.1 Binding of amylase to starch granules under non-hydrolysing conditions**

312 Interactions between amylase and starch granules require transportation of the amylase by
313 diffusion to the solid starch granules. The initial interaction (binding) of enzyme to starch
314 surfaces may involve (1) non-catalytic binding i.e. adherence of enzyme to the granule
315 surface by non-specific hydrogen bonding between OH groups of the starch moieties and
316 enzyme (protein) molecule or by Van der Waals interactions; or (2) catalytic binding i.e.

317 binding with at least 5 contiguous glucose residues in the active site of the enzyme
318 (Prodanov, Seigner & Marchis-Mouren, 1984; Seigner, Prodanov & Marchis-Mouren, 1987)
319 Initial binding can affect the subsequent catalytic events. If the binding occurs at the active
320 site, catalysis can proceed. Alternatively, if the binding is non-catalytic in nature, the overall
321 rate of enzyme action is decreased as enzyme molecules have to dissociate from the
322 nonspecific sites and return to solution before they can rebind to the starch substrate (Henis,
323 Yaron, Lamed, Rishpon, Sahar & Katchalski-Katzir, 1988). Measuring the concentration of
324 enzyme that is not bound to starch granules during the experiment conducted under non-
325 hydrolysing condition (usually 0 °C) has been used to determine the binding rates of amylase
326 to starch granules (Walker & Hope, 1963; Warren, Royall, Gaisford, Butterworth & Ellis,
327 2011). These experiments, however, represent an average of both catalytic and non-catalytic
328 binding over a population of granules.

329 The efficiency of enzyme adsorption has been previously reported to be inversely
330 proportional to the granule size, or, more precisely, to the surface area of the granules
331 (Schwimmer & Balls, 1949; Walker & Hope, 1963; Warren, Royall, Gaisford, Butterworth &
332 Ellis, 2011). The higher relative binding efficiency of smaller granules may be a factor
333 contributing to higher digestion rate of smaller starch granules naturally occurring in bulk
334 samples or obtained from fractionation of starches compared to larger granules (Dhital,
335 Shrestha & Gidley, 2010b; Tahir, Ellis & Butterworth, 2010).

336 Roughness and porosity at the surface of MS granules (Dhital, Shrestha & Gidley, 2010a), in
337 addition to increasing the available surface area, can also elevate the probability of catalytic

338 binding due to the presence of more accessible (available) starch molecules on exposed,
339 damaged, rough, and/or porous structures. The less organised regions are more accessible for
340 initial enzyme binding compared to regions with greater molecular order (Warren, Royall,
341 Gaisford, Butterworth & Ellis, 2011).

342 The enzyme preference towards some specific granules in both MS and PS is not apparently
343 related to granule size or surface area, and is therefore more likely to be governed by the
344 'available substrate' (starch chains that are sufficiently accessible as single chains to
345 potentially lead to catalytic binding) than the 'available surface area'. Based on the data
346 reported here, we propose that there can be localised variation in the amount of 'available
347 substrate' within or at the granule surface due to local polymer organisation factors, and that
348 enzyme binds preferentially to these specific regions of the granule. This is also evident in
349 **Figure 2**, where the preferential binding of enzyme to porous regions was observed. In
350 contrast, for granules without pores, enzyme was concentrated at the outer periphery similar
351 to non-treated starch (**Figure 1A**). The hilum (**Figure 2**, bold arrow) appeared to be the least
352 organised part of the granules since a relatively high proportion of enzyme was bound in the
353 hilum area within 5 min of incubation under non-hydrolysing condition.

354 The role of local surface structures in controlling the specificity of enzyme binding was
355 evident during double (consecutive) labelling experiments as shown in **Figure 1B** and
356 supplementary information **Figure S1** for MS, and **Figure 1D** and supplementary
357 information **Figure S3** for PS. The fresh enzyme bound at exactly the same granule sites that
358 had previously bound enzyme. The structural features associated with granules which bind
359 amylase compared to those which do not is the subject of current investigations.

360 **4.2 Amylolysis of starches**

361 The FITC-AA conjugate at 0.1, 0.4 and 0.8 units per mg of starch granules was used to study
362 the hydrolysis of starches with both A- (WMS, MS) and B- (PS, HAMS) type polymorphism.
363 The rate and extent of starch digestion were proportional to the concentration of enzyme
364 (**Figure 4**). As expected, the hydrolysis extent, at all enzyme concentrations, was highest in
365 WMS, followed by MS, PS and HAMS. The role of molecular, supra-molecular and granular
366 structures that affect the hydrolysis rate and extent of starch granules after initial binding has
367 been recently reviewed (Dhital, Warren, Butterworth, Ellis & Gidley, 2014). The electron
368 microscopic images of granule remnants after amylolysis with 0.8 unit FITC-AA conjugate
369 per mg of starch (**Figure 5, 6**, supplementary information **Figure S5** and **S6**) were in
370 agreement with several previous reports (Dhital, Shrestha & Gidley, 2010a, b; Planchot,
371 Colonna, Gallant & Bouchet, 1995; Zhang, Dhital & Gidley, 2013).

372 **4.3 Binding of amylase to starch granules at hydrolysing conditions**

373 For the first time, we have been able to localise amylase on starch granules during binding
374 and hydrolysis. Recently, Tawil *et al.* (2010) studied the location of bacterial amylase in
375 maize and waxy maize starches using light and synchrotron UV fluorescence microscopy
376 (measuring the auto-fluorescence of tryptophan in the enzyme). Starch samples were
377 incubated with enzyme under a microscope, and the changes in the granule morphology were
378 observed at different times. The experimental methodology employed by Tawil *et al.* (2010)
379 while highly innovative, was in some ways limited, as the authors were only able to visualise
380 one granule at a time, and the enzyme-starch interaction was observed under a microscope
381 coverslip, meaning that no mixing or temperature control could be employed. The present
382 study builds upon the findings of Tawil *et al.* (2010) by extending the study of the
383 localisation of enzyme during binding and hydrolysis of starch to starch samples from

384 multiple botanical origins, under a range of conditions, and with whole populations of
385 granules.

386 The adsorption of enzyme to starch granules during hydrolysis was found to be a highly
387 selective process. This selectivity is reflected in confocal microscopic images taken at
388 different digestion times (**Figure 7** and supplementary information **Figures S7, S8** and **S9**).
389 Similar to enzyme binding under non-hydrolysing conditions, after 5 min incubation under
390 hydrolysing conditions, the binding of FITC-AA conjugate to MS is more homogenous
391 compared to that of PS (**Figure 7** and supplementary information **Figure S7**). Confocal
392 microscopy observations of amylase binding to MS and WMS at different incubation times
393 (**Figure 7**, supplementary information **Figure S7, S8**) appear to confirm the usually accepted
394 ‘inside-out’ digestion pattern for A-polymorphic starches ascribed to the presence of pores
395 and channels that allow the easy diffusion of enzymes inside the granule to access the less
396 organised interior. However, the mere presence of surface pores and channels does not
397 necessarily mean that enzymes diffuse through them to the granule interior. In the present
398 study, it was observed that very few of the maize starch granules for which labelled dextran
399 was able to diffuse to their hilum, also showed diffusion of labelled enzyme to their hilum
400 (**Figure 3**).

401 In contrast to A-polymorphic WMS and MS (**Figure 7**, supplementary information **Figure**
402 **S7, S8**), the enzyme was bound only to selective granules in B-polymorphic starches (PS and
403 HAMS, **Figure 7** and supplementary information **Figure S7, S9**) during incubation under
404 hydrolysing conditions. This selectivity between granules and within granules would suggest
405 that the enzyme binding is restricted to sites on the starch granule surface that are suitable for
406 enzyme catalytic actions, as it is these regions that are subsequently degraded by enzyme,
407 while granules without enzyme bound are left untouched. Thus, the comparatively
408 homogenous binding of amylase under both non-hydrolysing and hydrolysing conditions in

409 MS suggests that the surface of maize starch contains more readily available substrates
410 possibly at the periphery of the pores. The enzyme initially catalytically binds at these
411 substrates and keeps hydrolysing with enlargement of pores (channels) until the enzyme can
412 access the less organised hilum region. After that, the enzyme starts hydrolysing from the
413 hilum towards the granule surface. In contrast, due to the absence of pores and channels in PS
414 and HAMS, amylase catalytically binds the granules that have a damaged surface or exposed
415 substrate and keep hydrolysing externally, so called 'exo-corrosion' (Dhital, Shrestha &
416 Gidley, 2010b). The inaccessibility of enzyme to the granule interior further suggests that the
417 surface structure of PS and HAMS is rate limiting to the hydrolysis of these starches.

418 **5 Conclusion**

419 This study shows that amylase binds to starch granules in selected local regions under both
420 hydrolysing and non-hydrolysing conditions. It is proposed that binding occurs to those
421 regions which have less local molecular order and therefore contain abundant potential
422 binding sites for α -amylase. Once bound, subsequent catalytic action exposes more potential
423 binding sites, thus granule digestion becomes comparatively easier during digestion, resulting
424 in extensive digestion of some granules in the presence of limited if any digestion of other
425 granules. The different behaviour of α -amylase to dextran probes of similar size suggests that
426 physical accessibility is not the determinant for enzyme localisation, and that therefore
427 binding interactions are more likely to be the most important factor in determining the
428 specificity of enzyme location.

429

430 **Acknowledgements**

431

432 This work was supported in part by the Australian Research Council (Discovery Grant DP130102461)
433 and a University of Queensland Postdoctoral Fellowship awarded to FW. We acknowledge the

434 facilities, and the scientific and technical assistance of the Australian Microscopy & Microanalysis
435 Research Facility at the Centre for Microscopy and Microanalysis, The University of Queensland.

436 **References**

437 Apinan, S., Yujiro, I., Hidefumi, Y., Takeshi, F., Myllärinen, P., Forssell, P., & Poutanen, K.
438 (2007). Visual observation of hydrolyzed potato starch granules by α -amylase with Confocal
439 Laser Scanning Microscopy. *Starch/Stärke*, 59(11), 543-548.

440 Dhital, S., Shelat, K., Shrestha, A. K., & Gidley, M. J. (2013). Heterogeneity in maize starch
441 granule internal architecture deduced from diffusion of fluorescent dextran probes.
442 *Carbohydrate Polymers*, 93, 365– 373.

443 Dhital, S., Shrestha, A. K., & Gidley, M. J. (2010a). Effect of cryo-milling on starches:
444 Functionality and digestibility. *Food Hydrocolloids*, 24(2), 152-163.

445 Dhital, S., Shrestha, A. K., & Gidley, M. J. (2010b). Relationship between granule size and *in*
446 *vitro* digestibility of maize and potato starches. *Carbohydrate Polymers*, 82(2), 480-488.

447 Dhital, S., Warren, F. J., Butterworth, P. J., Ellis, P. R., & Gidley, M. J. (2014). Mechanisms
448 of starch digestion by α -amylase – structural basis for kinetic properties. *Critical Reviews in*
449 *Food Science and Nutrition*, accepted for publication.

450 Gallant, D. J., Bouchet, B., & Baldwin, P. M. (1997). Microscopy of starch: Evidence of a
451 new level of granule organization. *Carbohydrate Polymers*, 32(3), 177-191.

452 Helbert, W., Schülein, M., & Henrissat, B. (1996). Electron microscopic investigation of the
453 diffusion of *Bacillus licheniformis* α -amylase into corn starch granules. *International journal*
454 *of Biological Macromolecules*, 19(3), 165-169.

455 Henis, Y. I., Yaron, T., Lamed, R., Rishpon, J., Sahar, E., & Katchalski - Katzir, E. (1988).
456 Mobility of enzymes on insoluble substrates: The β amylase-starch gel system. *Biopolymers*,
457 27(1), 123-138

458 Huber, K. C., & BeMiller, J. N. (1997). Visualization of channels and cavities of corn and
459 sorghum starch granules. *Cereal Chemistry*, 74(5), 537-541.

- 460 Jane, J. L., & Shen, J. J. (1993). Internal structure of the potato starch granule revealed by
461 chemical gelatinization. *Carbohydrate Research*, 247, 279-290.
- 462 Liu, D., Parker, M. L., Wellner, N., Kirby, A. R., Cross, K., Morris, V. J., & Cheng, F.
463 (2013). Structural variability between starch granules in wild type and in *ae* high-amylose
464 mutant maize kernels. *Carbohydrate Polymers*, 97(2), 458-468.
- 465 Leach, H. W., & Schoch, T. J. (1961). Structure of the starch granule. II. Action of various
466 amylases on granular starches. *Cereal Chemistry*, 38(1), 34-36.
- 467 Lynn, A., & Cochrane, M. P. (1997). An evaluation of confocal microscopy for the study of
468 starch granule enzymic digestion. *Starch/Stärke*, 49(3), 106-110.
- 469 Moretti, R., & Thorson, J. S. (2008). A comparison of sugar indicators enables a universal
470 high-throughput sugar-1-phosphate nucleotidyltransferase assay. *Analytical Biochemistry*,
471 377(2), 251-258.
- 472 Pan, D. D., & Jane, J. L. (2000). Internal structure of normal maize starch granules revealed
473 by chemical surface gelatinization. *Biomacromolecules*, 1(1), 126-132.
- 474 Planchot, V., Colonna, P., Gallant, D. J., & Bouchet, B. (1995). Extensive degradation of
475 native starch granules by α -amylase from *Aspergillus fumigatus*. *Journal of Cereal Science*,
476 21(2), 163-171.
- 477 Prodanov, E., Seigner, C., & Marchis-Mouren, G. (1984). Subsite profile of the active center
478 of porcine pancreatic α -amylase. Kinetic studies using maltooligosaccharides as
479 substrates. *Biochemical and Biophysical Research Communications*, 122(1), 75-81.
- 480 Schwimmer, S., & Balls, A. (1949). Starches and their derivatives as adsorbents for malt α -
481 amylase. *Journal of Biological Chemistry*, 180(2), 883-894.
- 482 Seigner, C., Prodanov, E., & Marchis-Mouren, G. (1987). The determination of subsite
483 binding energies of porcine pancreatic α -amylase by comparing hydrolytic activity towards
484 substrates. *Biochimica et Biophysica Acta (BBA)-Protein Structure and Molecular*
485 *Enzymology*, 913(2), 200-209.

- 486 Sujka, M., & Jamroz, J. (2009). α -Amylolysis of native potato and corn starches—SEM, AFM,
487 nitrogen and iodine sorption investigations. *LWT-Food Science and Technology*, 42(7), 1219-
488 1224.
- 489 Tahir, R., Ellis, P. R., & Butterworth, P. J. (2010). The relation of physical properties of
490 native starch granules to the kinetics of amylolysis catalysed by porcine pancreatic α -
491 amylase. *Carbohydrate Polymers*, 81(1), 57-62.
- 492 Tawil, G., Jamme, F., Réfrégiers, M., Viksø-Nielsen, A., Colonna, P., & Buléon, A. (2010).
493 *In situ* tracking of enzymatic breakdown of starch granules by synchrotron UV fluorescence
494 microscopy. *Analytical Chemistry*, 83(3), 989-993.
- 495 The, T. H., & Feltkamp, T. E. W. (1970). Conjugation of fluorescein isothiocyanate to
496 antibodies: I. Experiments on the conditions of conjugation. *Immunology*, 18(6), 865 - 873.
- 497 Thomson, N., Miles, M., Ring, S., Shewry, P., & Tatham, A. (1994). Real - time imaging of
498 enzymatic degradation of starch granules by atomic force microscopy. *Journal of Vacuum
499 Science & Technology B: Microelectronics and Nanometer Structures*, 12(3), 1565-1568.
- 500 Walker, G. J., & Hope, P. M. (1963). The action of some α -amylases on starch granules.
501 *Biochemical Journal*, 86(3), 452- 462
- 502 Warren, F. J., Royall, P. G., Gaisford, S., Butterworth, P. J., & Ellis, P. R. (2011). Binding
503 interactions of α -amylase with starch granules: The influence of supramolecular structure and
504 surface area. *Carbohydrate Polymers*, 86(2), 1038-1047.
- 505 Zhang, B., Dhital, S., & Gidley, M. J. (2013). Synergistic and antagonistic effects of α -
506 amylase and amyloglucosidase on starch digestion. *Biomacromolecules*, 14 (6), 1945–1954.
507

507

508 **Figure Captions**

509 **Figure 1A:** Confocal (first and third column) and differential interference contrast (second
510 and fourth column) images of bound FITC- and TRITC-AA conjugate on maize starch
511 granules incubated for 5 and 20 minutes at 0 °C.

512 **Figure 1B:** Confocal (top panel) and differential interference contrast (bottom panel) images
513 of bound FITC- and TRITC-AA conjugate on maize starch granules incubated for 25 min at 0
514 °C. TRITC-AA conjugate, 8 units per mg of starch, was added after 20 min incubation of
515 FITC-AA conjugate.

516 **Figure 1C:** Confocal (first and third column) and differential interference contrast (second
517 and fourth column) images of bound FITC- and TRITC-AA conjugate on potato starch
518 granules incubated for 5 and 20 min at 0 °C.

519 **Figure 1D:** Confocal (top panel) and differential interference contrast (bottom panel)
520 images bound FITC- and TRITC-AA conjugate on potato granules incubated for 25 min at 0
521 °C. TRITC-AA conjugate, 8 unit pre mg of starch, was added after 20 min incubation of
522 FITC-AA conjugate.

523 **Figure 2:** Electron, confocal and differential interference contrast images of porous granules.
524 A: Electron microscopic picture of maize starch granules incubated with non-labelled AA for
525 20 min at 37 °C. B, C, and D: Confocal microscopic and differential interference contrast
526 images of porous granules bound with FITC-AA conjugate for 5 min at 0 °C.

527 **Figure 3:** Confocal and differential interference contrast images of diffused dextran probes
528 and initial amylolysis of maize starch granules with diffused dextran probes. A: Maize starch
529 granules (differential interference contrast image), B and C: confocal and differential
530 interference contrast images of diffused dextran probes inside the maize starch granules after
531 overnight incubation. D, E: confocal image after 5 min of amylolysis by FITC-AA conjugate.
532 F: Differential interference contrast image after 5 min of amylolysis by FITC-AA conjugate.

533 **Figure 4:** FITC-AA conjugate catalysed hydrolysis rate of starches; waxy maize (WMS),
534 maize (MS), potato (PS), high amylose maize- Gelose 80 (HAMS). A, B, and C represents
535 the digestogram at 0.1, 0.4 and 0.8 unit of FITC-AA conjugate per mg of starch.

536 **Figure 5:** Electron microscopic images of un-hydrolysed maize starch granules and granule
537 remnant after hydrolysis for 5 min, 30 min, 2 h, 4 h and 24 h with 0.8 unit FITC-AA
538 conjugate per mg of starch.

539 **Figure 6:** Electron microscopic images of un-hydrolysed potato starch granules and granule
540 remnant after hydrolysis for 5 min, 30 min, 2 h, 4 h and 24 h with 0.8 unit FITC-AA
541 conjugate per mg of starch.

542 **Figure 7:** Confocal (first and third column) and differential interference contrast (second and
543 third column) images of maize (MS) and potato (PS) starch granule remnants after hydrolysis
544 for 5 min, 30 min, 2 h, 4 h and 24 h with 0.8 unit FITC-AA conjugate per mg of starch.

545

546

547

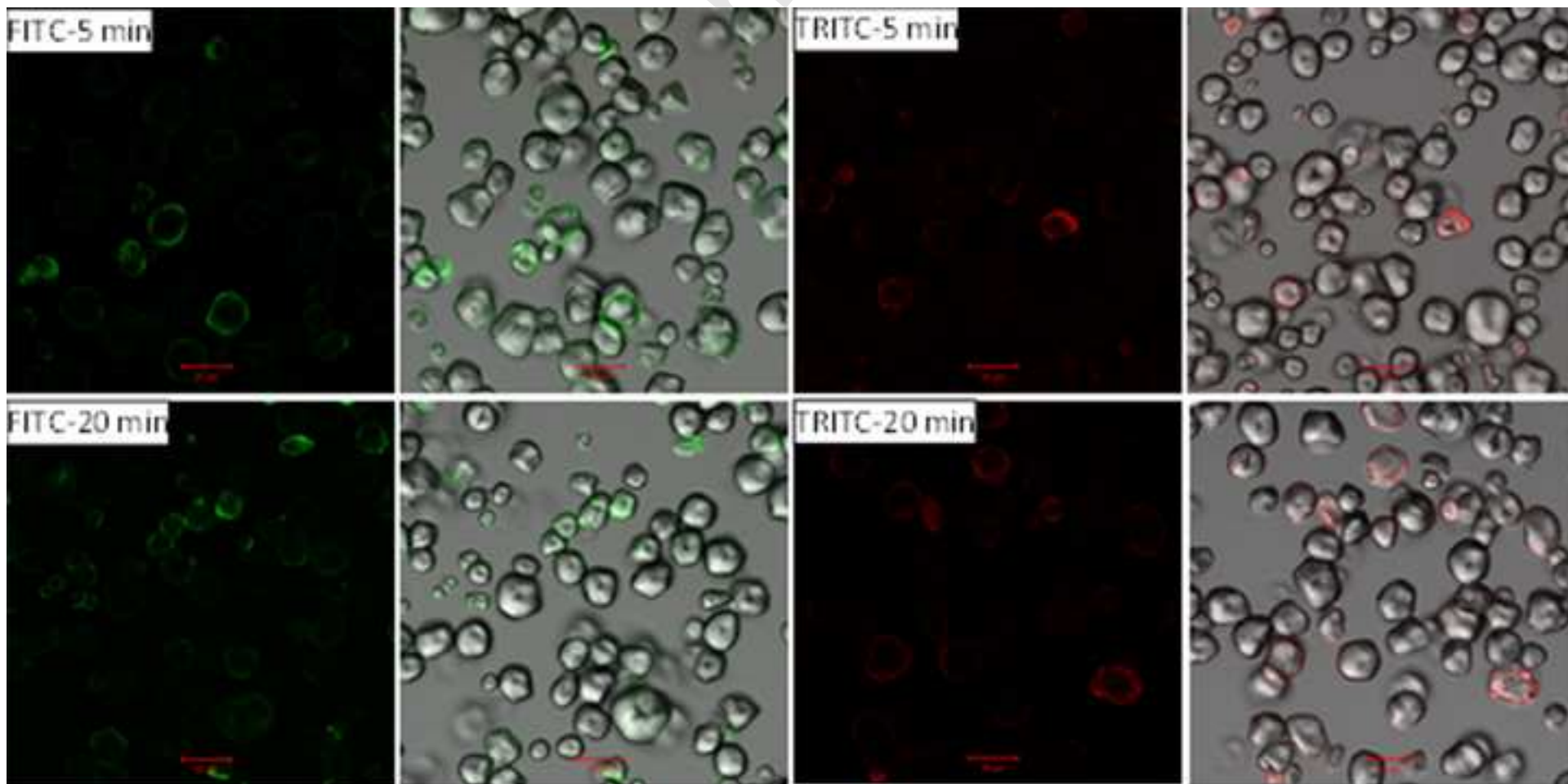
548

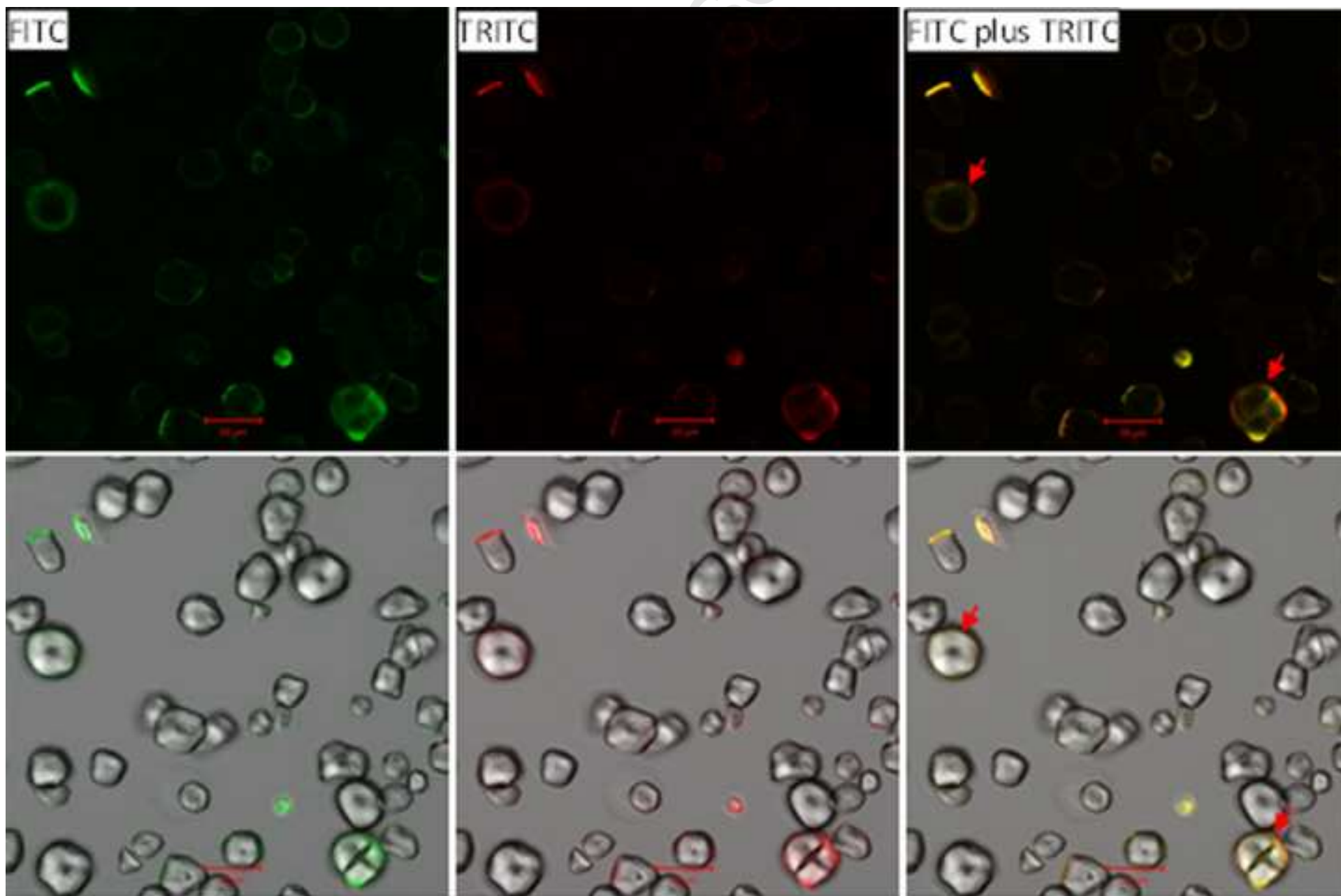
Highlights

- Alpha-amylase labelled using two fluorophores with retention of activity
- Confocal localisation of enzymes under non-hydrolysing and hydrolysing conditions
- Enzymes bind preferentially to selected regions of only some granules
- Hydrolysis occurs first in those regions associated with bound enzyme
- No correlation between dextran accessibility and sites of enzyme binding

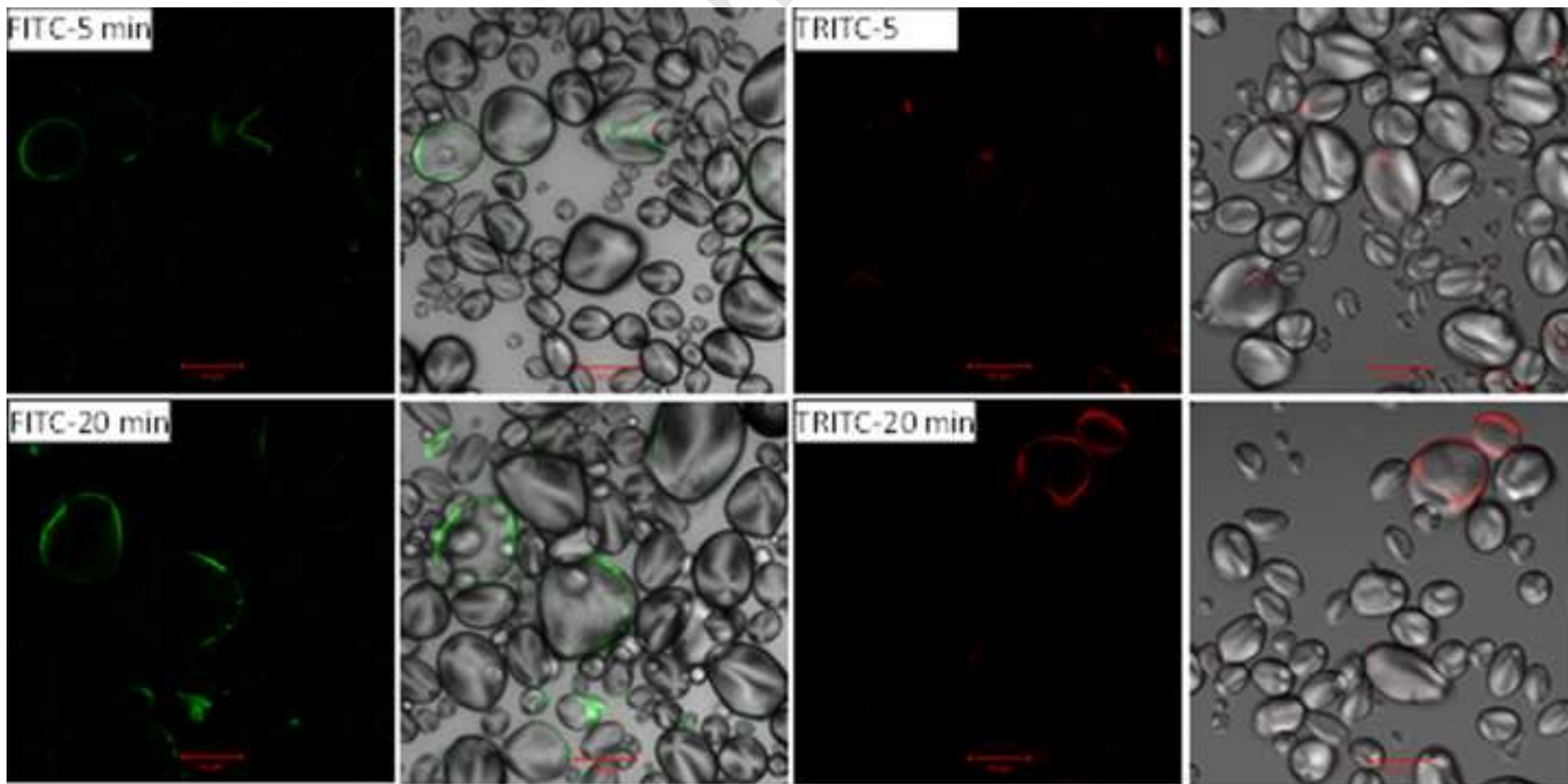
Accepted Manuscript

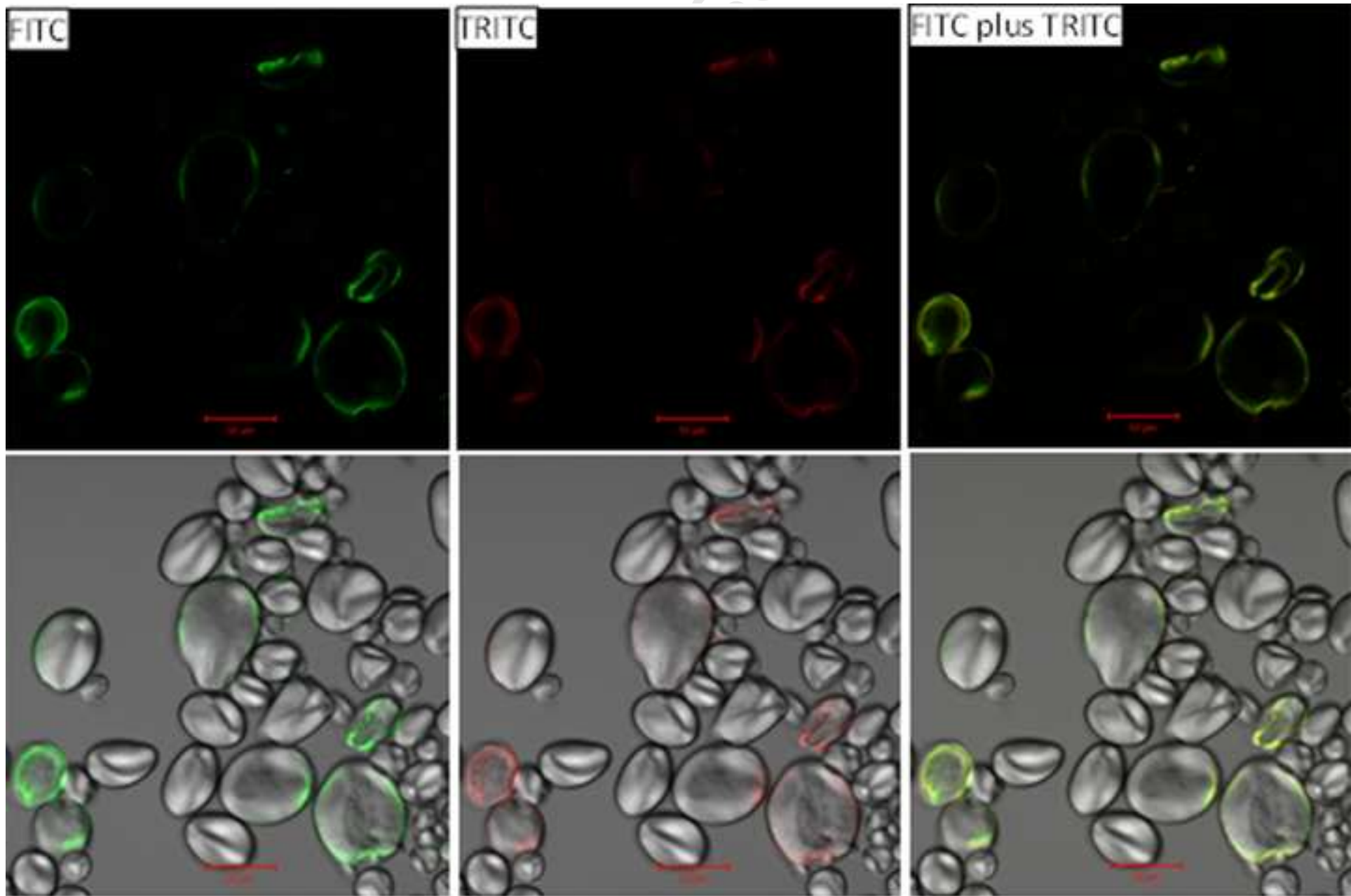
Manuscript

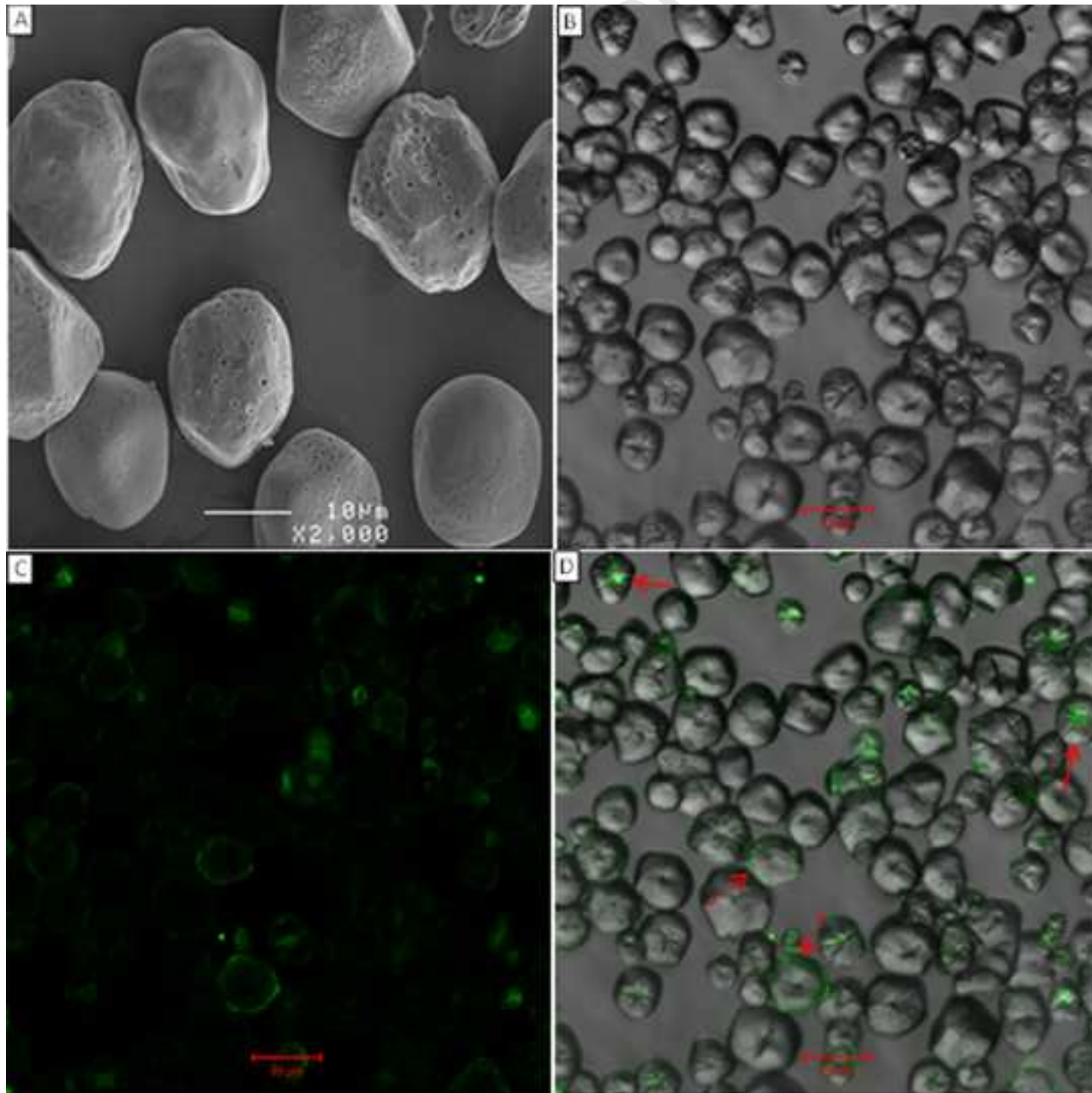


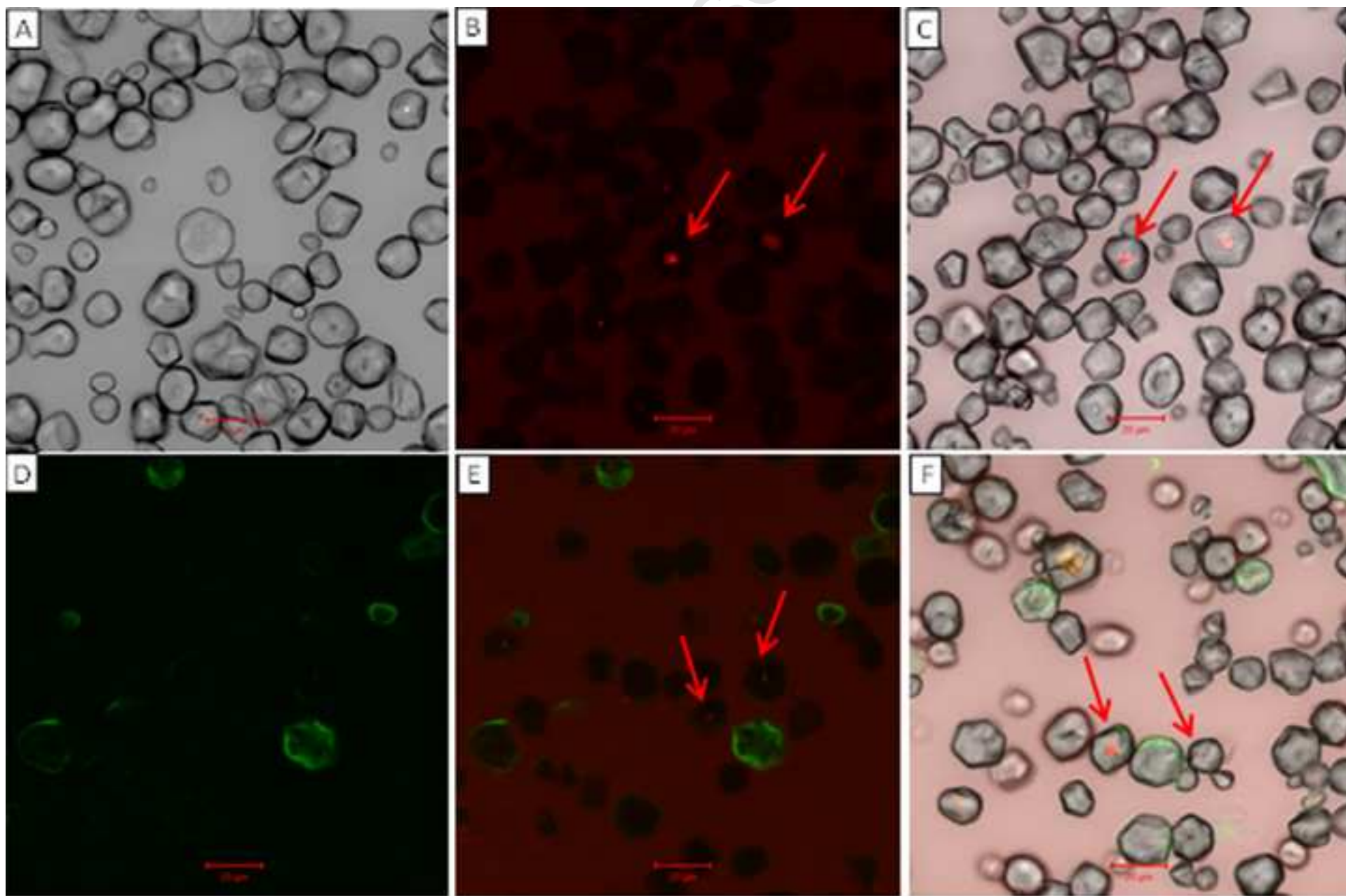


Manuscript

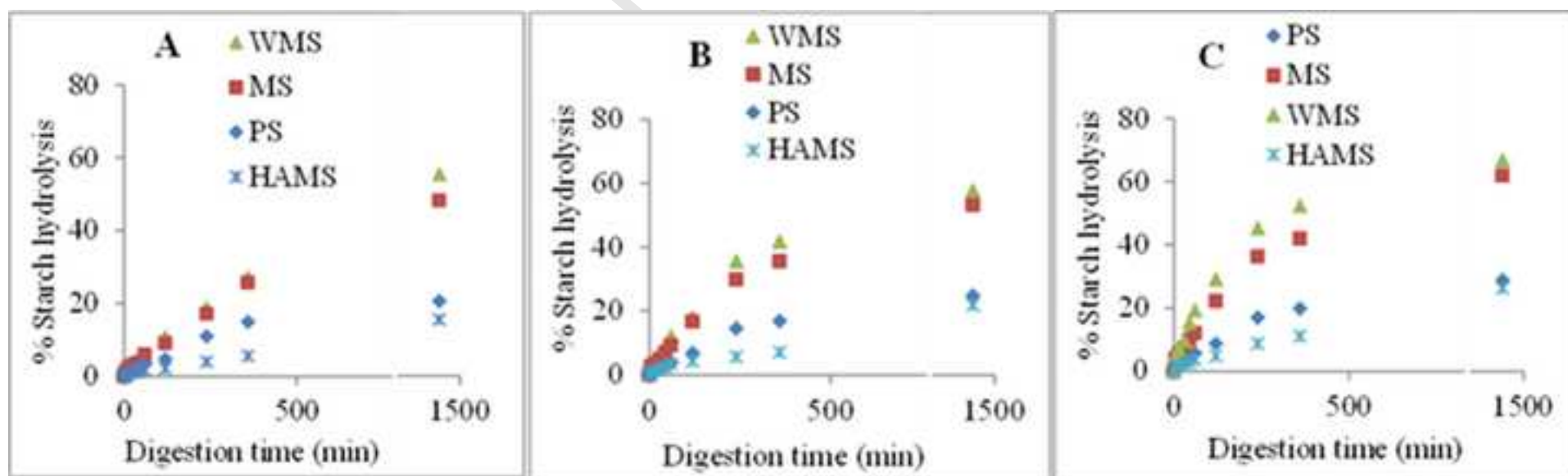




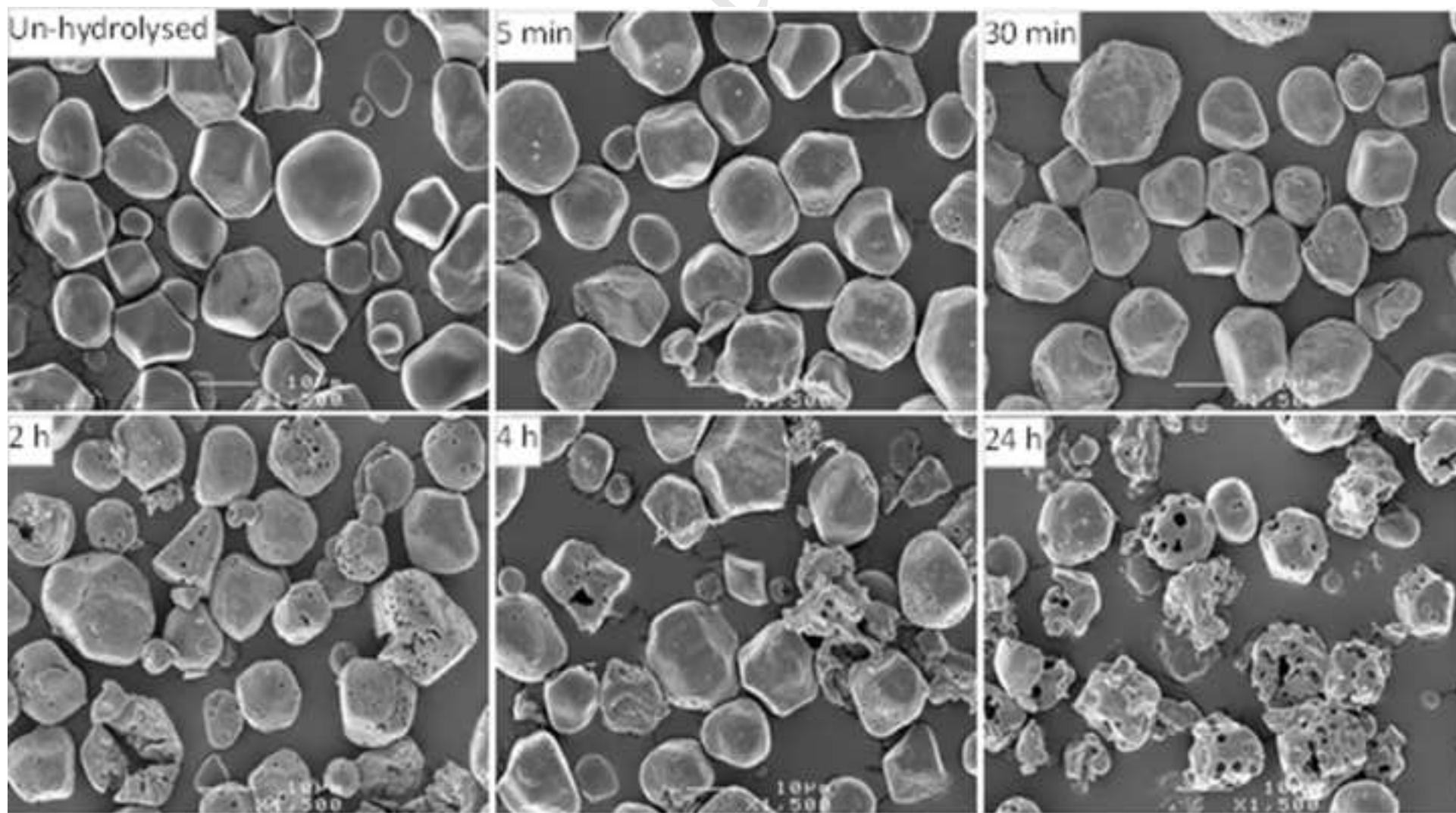




Manuscript



USCrip



USCrip

